

Published in final edited form as:

*Arterioscler Thromb Vasc Biol.* 2013 January ; 33(1): 76–86. doi:10.1161/ATVBAHA.112.251736.

## Transcriptome analysis for Notch3 target genes identifies Grip2 as a novel regulator of myogenic response in the cerebrovasculature

Charles Fouillade<sup>1,2</sup>, Céline Baron-Menguy<sup>1,2</sup>, Valérie Domenga-Denier<sup>1,2</sup>, Christelle Thibault<sup>3</sup>, Kogo Takamiya<sup>4</sup>, Richard Huganir<sup>5</sup>, and Anne Joutel<sup>1,2</sup>

<sup>1</sup>INSERM, U740, Paris, F-75010, France

<sup>2</sup>Univ Paris Diderot, Sorbonne Cité, UMR S740, Paris, F-75010, France

<sup>3</sup>Institut de Génétique et de Biologie Moléculaire (IGBMC), Illkirch, France

<sup>4</sup>Department of Neuroscience; Faculty of Medicine, Graduate School of Medicine; UNIVERSITY of MIYAZAKI; 5200 Kihara Kiyotake Miyazaki, JAPAN

<sup>5</sup>Department of Neuroscience and Howard Hughes Medical Institute, Johns Hopkins University School of Medicine, Hunterian 1001, 725 N. Wolfe Street, Baltimore, MD 21205, USA

### Abstract

**Objective**—Notch3 is critically important for the structure and myogenic response of distal arteries, particularly of cerebral arteries. However, signaling pathways acting downstream of Notch3 remain largely unknown.

**Methods and results**—Transcriptome analysis using tail arteries of Notch3-null mice identified a core set of 17 novel Notch3-regulated genes confirmed in tail or brain arteries. Post-natal deletion of RBP-J $\kappa$  in smooth muscle cells recapitulated the structural, functional and molecular defects of brain arteries induced by Notch3 deficiency. Transient *in vivo* blockade of the Notch pathway with  $\gamma$ -secretase inhibitors uncovered, in addition to *Notch3*, six immediate responders including the voltage-gated potassium channel Kv1.5, which opposes to myogenic constriction of brain arteries, and the glutamate receptor interacting protein 2 (GRIP-2), with no previously established role in the cerebrovasculature. We identified a vascular smooth muscle cell isoform of *Grip2*. We showed that Notch3-RBP-J $\kappa$  specifically regulates this isoform. Finally, we found that cerebral arteries of Grip2 mutant mice, which express a N-terminally truncated GRIP-2 protein, exhibited selective attenuation of pressure-induced contraction.

**Conclusion**—Our data provide insight into how Notch3 signals in the brain arteries, establishing the postnatal requirement of smooth muscle RBP-J $\kappa$  in this context. Notch3-regulated transcriptome provides potential for modulating myogenic response in the cerebrovasculature.

### Keywords

Notch3; cerebrovasculature; myogenic response; smooth muscle cell; transcriptome

---

Correspondence should be addressed to Anne JOUTEL (Faculté de Médecine Paris Diderot, site Villemin, 10 av de Verdun, 75010 Paris, France; Tel 331 57278593, Fax 331 57278594, anne.joutel@univ-paris-diderot.fr).

Fouillade, Notch3 target genes in distal arteries

### Disclosures

None

Distal arteries are muscular arteries of small diameter and high resistance. Their wall is composed of one or a few layers of smooth muscle cells (SMC) that confer the myogenic response, which refers to the property these arteries have to modulate their diameter in response to changes in intravascular pressure. Myogenic response involves a graded SMC depolarization, which activates L-type voltage-dependent calcium (Ca<sup>2+</sup>) channels, leading to elevation of the cytosolic Ca<sup>2+</sup> concentration, SMC contraction, and vasoconstriction. Myogenic reactivity is key in the setting of vascular resistance and local control of microvascular blood flow<sup>1</sup>. It is particularly well developed in brain arteries where it is a major contributor to the maintenance of cerebral blood flow during variations in systemic blood pressure<sup>2</sup>. In humans, small-artery-disease of the brain accounts for more than 25 % of strokes and is a leading cause of cognitive decline and disability<sup>3</sup>.

The Notch signaling pathway is an evolutionarily conserved, intercellular signaling mechanism that plays a critical role in the development and homeostasis of blood vessels<sup>4</sup>. Endothelial Notch signaling is required for several critical steps in angiogenesis including arterial-venous specification, tip cell differentiation as well as growth and stability of the blood vessel network<sup>5</sup>. Also, Notch signaling positively regulates multiple aspects of vascular SMC (vSMC) specification, differentiation and maturation. There are 4 Notch receptors (Notch 1 to 4) in mammals but several lines of evidence indicate that Notch3, which is predominantly expressed in vSMC, is the key Notch receptor in distal arteries, and particularly in the brain arteries<sup>6</sup>. Targeted mutagenesis that disrupts *Notch3* in the mouse results in a failure of arterial differentiation and maturation of vSMC in distal arteries including the cerebral arteries<sup>7</sup>. Mice deficient for Notch signaling in vSMC or lacking Notch3 exhibit profound defects in cerebrovascular patterning<sup>8,9</sup>. Notch3 deficiency strongly impacts myogenic tone of distal arteries, and particularly of brain arteries<sup>10</sup>. This results in strongly compromised autoregulation of cerebral blood flow and increased susceptibility to ischemic stroke upon challenge<sup>7,11</sup>. Importantly, dominant mutations of *NOTCH3* cause CADASIL, an adult onset small-vessel-disease of the brain in humans<sup>12</sup>.

In response to ligand activation, Notch receptors undergo a series of proteolytic cleavages resulting in the release of the Notch intracellular domain (NICD) from the plasma membrane. After translocation to the nucleus, NICD binds to the transcription factor RBP-J $\kappa$  and coactivator Mastermind to activate transcription of genes by turning RBP-J $\kappa$  from a repressor to an activator<sup>13</sup>. Alternatively, in some forms of non-canonical signaling, Notch activation can trigger cellular responses without the involvement of RBP-J $\kappa$ <sup>14,15</sup>. Importantly, there is a major diversity in the immediate downstream Notch response as revealed by the analysis of Notch-induced transcriptomes in different cellular types and contexts<sup>16,17</sup>.

The downstream mechanisms of Notch3 signaling in the context of distal arteries, and particularly of brain arteries, remain poorly known. The *Hes* and *Hey* genes, the most well characterized immediate Notch target genes, are unchanged in distal arteries of Notch3 null mice<sup>18</sup>. So far, only a few Notch downstream effectors, including Platelet-Derived Growth Factor Receptor- $\beta$  receptor and integrin  $\beta$ 3, have been shown to be involved in maturing small arteries<sup>19,20</sup>.

To explore the molecular mechanisms acting downstream of Notch3, we used a combination of mouse models with constitutive deletion of Notch3, inducible deletion of RBP-J $\kappa$  in SMC or transient pharmacological blockade of the Notch pathway to carry out transcriptome analysis and quantitative RT-PCR on isolated distal arteries. Herein, we report the identification of a core set of novel Notch3-RBP-J $\kappa$  regulated genes, including immediate and persistent responders of importance for brain artery function. As an example, we

uncover for the first time to our knowledge the Glutamate interacting protein 2 as a regulator of myogenic activity in the cerebrovasculature.

## Methods

An expanded version is provided in the Supplemental material.

### Animal studies

The Notch3<sup>-/-</sup> (C57BL/6J)<sup>7</sup>, RBP-J $\kappa$ <sup>fllox/fllox</sup> (C57BL/6J)<sup>21</sup>, SMMHC-Cre<sup>ERT2</sup> (C57BL/6J)<sup>22</sup>, NAS (C57BL/6J)<sup>18, 23</sup> and Grip2 mutant<sup>24</sup> lines (C57BL/6J) have been described previously. SM-RBP-J-KO mice were generated by cross-breeding RBP-J<sup>fllox/fllox</sup> with SMMHC-Cre<sup>ERT2</sup> mice, deletion was induced at post natal day 1 by intragastric injection of tamoxifen. SMMHC-Cre<sup>ERT2</sup> mice crossed with Rosa26-Stopfl-LacZ reporter mice<sup>25</sup> were used to monitor tamoxifen-induced Cre/Lox recombination (Supplemental Figure I). Transient Notch pathway blockade was achieved by intraperitoneal injection of the  $\gamma$ -secretase inhibitor LY-411575 (kind gift from Dr. Todd Golde) to sort out, within the list of genes regulated by Notch3/RBP-J $\kappa$ , those which quickly respond to Notch inhibition. The experimental procedures conformed to the national guidelines for the use of animals in research and were approved by the Ethics committees on animal experiment (regional committee of Paris, Ile de France n°4 and local committee of University Paris Diderot, Lariboisière-Villemin).

### Gene expression analysis

Caudal artery cRNAs were hybridized to Mouse Genome 430 2.0 oligonucleotide arrays at the IGBMC microarray Core Facility. Array data were processed using Gene Chip operating Software (GCOS v1, Affymetrix, Santa Clara, CA, USA) and analysis of gene expression profiles was done using Robust Multichip Average<sup>26</sup>. Student's t-test was used to evaluate differential expression, the Westfall-Young permutation method was used to perform multiple test correction (resampling pValue). The array data are available at Gene expression Omnibus at the National Center for Biotechnology Information (accession no. GSE36437).

Quantitative RT-PCR analysis was performed on a MyiQ<sup>TM</sup> Single-Color Real-Time PCR detection system (Biorad) as previously described<sup>18</sup>.

In situ hybridization was performed on paraffin sections from embryos and adult C57Bl/6J wild-type mice using Grip2 and Notch3 antisense cRNA probes as described previously<sup>7</sup>.

### Histological analysis

Whole-mount staining for  $\beta$ -galactosidase activity was performed as described<sup>18</sup>. The middle cerebral artery was examined by high resolution optical microscopy on semi-thin sections and electron microscopy on ultra-thin sections as described previously<sup>18</sup>. Frozen brain sections were stained with rabbit anti-Grip2C polyclonal antibody<sup>27</sup> and mouse anti- $\alpha$ -smooth muscle actin ( $\alpha$ -SMA) monoclonal antibody (clone A4, Dako). Paraffin sections were stained with rabbit anti-smooth muscle myosin heavy chain polyclonal antibody (Biomedical Technologies Inc.)

### Vascular reactivity analysis

Segments of the posterior cerebral artery or caudal artery were isolated from Grip2 mutant male mice, SM-RBPJ-KO mice and wild-type littermates and mounted in a video monitored perfusion system (Living Systems Instrumentation) as previously described<sup>28</sup>.

Vasoreactivity to Acetylcholine (Ach), Phenylephrine (PE) and Potassium Chloride (KCl)

was examined on pressurized (50 mmHg) vessels. Myogenic tone was measured by increasing intraluminal pressure by steps from 10 to 100 mmHg.

### Statistical analysis

Data are expressed as mean  $\pm$  Standard error of the mean (sem). Two-group comparisons were analyzed by the two-tailed t-test for independent samples. Multiple comparisons were evaluated by 1-factor ANOVA followed by the Bonferroni post-hoc test. P values of  $<0.05$  were considered significant.

## Results

### Notch3-dependent transcriptome in distal arteries

In an attempt to identify genes that serve as downstream effectors of Notch3 in the context of maturing distal artery, we compared the gene expression profile of arteries from Notch3<sup>-/-</sup> (Notch3KO) and wild-type (WT) mice by a RNA microarray analysis. The caudal artery was collected at one month of age, the final stage of artery maturation. Of the ~30,000 known genes arrayed on the chip, about 36 % were present in the wild-type arteries. A total of 188 distinct probe sets, corresponding to 159 transcripts, were identified as differentially regulated in the mutant ( $>1.5$ -fold change,  $P<0.05$ ) compared to control arteries. Among these, 103 transcripts were found upregulated and 56 downregulated (Supplemental Table I).

Since Notch receptors function as transcriptional activators we prioritized the group of downregulated genes. When we applied to this group of genes a further selection step, a stringent pairwise comparison, the number of genes of interest was narrowed down to 17. We next validated the microarray results by quantitative RT-PCR (QRT-PCR) analysis in independently obtained caudal artery RNA samples (n=4 per genotype) and in a set of brain artery RNA samples (n=3 per genotype) collected in one month-old Notch3KO and WT mice. The QRT-PCR results showed that all of these were downregulated in Notch3KO caudal or brain arteries confirming the validity of our microarray approach (Table 1). Sixteen of these genes were significantly downregulated in the Notch3KO caudal arteries, most of them at fold ratios comparable to those in the global gene profile, and 15 were downregulated in the Notch3KO brain arteries.

Among these 17 Notch3-regulated genes, 3 genes (*Pln* (phospholamban), *S1pr3* (sphingosine-1-phosphate receptor 3), and *Kvl.5* (potassium voltage-gated channel, shaker-related subfamily, member 5) have an established role in the regulation of arterial tone or SMC function<sup>29-31</sup>. Two other genes (*Cdh6* (cadherin-6) and *Ptp4a3* (protein-tyrosine phosphatase 4a3)) have documented expression in the vasculature<sup>32,33</sup>. The subset of 15 genes, identified as downregulated in the Notch3KO brain arteries, was chosen for further characterization.

### Post-natal deletion of RBP-J $\kappa$ in SMC recapitulates structural defects, functional alterations and molecular changes of brain arteries induced by loss of Notch3

We first investigated the requirement of smooth muscle RBP-J $\kappa$  for the expression of Notch3 target genes. We generated mice with SMC-deletion of RBP-J $\kappa$  (SM-RBP-J-KO), by mating a conditional allele of RBP-J $\kappa$  (*RBP-J<sup>fllox</sup>*)<sup>21</sup> with a tamoxifen-inducible CreER driver mouse line (SMMHC-CreER<sup>T2</sup>), which expresses an inducible Cre recombinase under the control of the smooth muscle myosin heavy chain promoter<sup>22</sup>. Our previous work suggested that, in distal arteries, Notch3 operates in the postnatal period<sup>7</sup>. Consequently, we induced deletion of RBP-J $\kappa$  immediately after birth (Supplemental Figure I).

Morphological inspection of the brain from 1 month-old mice revealed strong enlargement of the arteries in SM-RBP-J-KO mice (n=5) as compared to control mice (n=6). High-resolution optic microscopy analysis showed marked thinning of SMC, dilation of mutant arteries with a less festooned elastica lamina (Figure 1A–D and G). Remarkably, immunostaining for smooth muscle myosin heavy chain, a common marker of contractile SMC, was roughly preserved in mutant brain arteries (Figure 1 E,F). Overall, arterial defects of SM-RBP-J-KO resembled those of Notch3KO mice at the histological level (Supplemental Figure II). Moreover, SM-RBP-J-KO mice (n=6) exhibited strongly reduced myogenic tone within the cerebral arteries as compared to control mice (n=5 *RBP-J $\kappa$ <sup>fllox/fllox</sup>* treated with tamoxifen) (Figure 1H). Of note, ACh-induced dilation and PE or KCl-induced contractile responses were also attenuated in mutant arteries (Supplemental Figure III).

Importantly, 13 out of the 15 Notch3-regulated genes tested were found to be significantly downregulated in SM-RBP-J-KO brain arteries (n= 4 samples) as compared to control arteries (n= 5 samples from *RBP-J $\kappa$ <sup>fllox/fllox</sup>* littermates treated with tamoxifen and 4 samples from *RBP-J $\kappa$ <sup>fllox/fllox</sup>, SMMHC-CreER<sup>T2</sup>* treated with vehicle) (Figure 1H). Thus, these data establish the post-natal requirement of smooth muscle RBP-J $\kappa$  for proper maturation of distal arteries and indicate that, in this context, Notch3 signaling conforms to the canonical RBP-J $\kappa$  pathway.

### Categorization of Notch3-RBP-J $\kappa$ downregulated genes

The list of genes identified as downregulated in brain arteries of Notch3KO and SM-RBP-J-KO mice likely includes a combination of immediate and late targets as well as genes whose change correspond to physiological adaptation. To discriminate between these distinct classes of genes and pinpoint the immediate targets we assessed mRNAs expression level in the brain arteries upon transient blockade of the Notch pathway. Mice were treated by  $\gamma$ -secretase inhibitors (GSI), which inhibit the cleavage releasing the NICD from the plasma membrane required for Notch signaling, for 3 to 5 consecutive days. To control for efficient Notch pathway blockade, we used the NAS line, which expresses the  $\beta$ -galactosidase gene under the control of a minimal promoter containing multiple RBP-J $\kappa$  response elements, and monitored expression level of  $\beta$ -galactosidase mRNA upon GSI treatment<sup>18</sup>. Diminished expression of  $\beta$ -galactosidase mRNA was detected in the brain arteries of GSI treated mice as early as the third day and decreased expression reached statistical significance at day 5. Of interest, *Notch3*, which expression is dependent on Notch signaling<sup>34</sup>, was also significantly downregulated from the 3<sup>rd</sup> day of GSI treatment (Figure 2A).

Of the 15 Notch3-regulated genes tested, six genes were found to be downregulated upon GSI treatment while the others showed either no change or opposite trends (Figure 2B and supplemental Table II). *Nrip2* and *Pgam2* were significantly downregulated from day 3, and decreased expression of these 2 genes was further accentuated at day 5. *Grip2* and *Kv1.5* had their transcript level also decreased from day 3, but downregulation of these 2 genes reached statistical significance at day 5. The latter genes, *Susd5* and *Xirp1*, showed significant downregulation only upon 5 days of GSI treatment. Thus the quick response to *in vivo* Notch inactivation of these genes is consistent with the possibility that these 6 genes be immediate targets.

### Grip2 is expressed in SMC of distal arteries

Further analysis focused on the characterization of *Grip2*, which displayed pronounced downregulation upon genetic and pharmacological inactivation of the Notch pathway. *Grip2* encodes a 130-kDa multi-PDZ domain-containing protein, highly enriched in the brain. It belongs to a small family of cytoplasmic scaffolding proteins (GRIP-1 and GRIP-2) known to interact with AMPA-type glutamate receptor and to regulate its trafficking<sup>35, 36</sup>. Vascular



expression and function of GRIP-2 have not been reported yet. Significantly, subunits of the AMPA receptors that interact with GRIP-2, have negligible expression in the brain arteries (Supplemental Figure IV). Therefore, we first analyzed expression pattern of *Grip2* in detail. *In situ* hybridization showed *Grip2* to be robustly expressed in the murine brain vessels, in addition to neurons, from post-natal day 1 and in adults (Figure 3 A,D). *Grip2* mRNA was also detected in the vessels of other organs, including the kidney, heart, skeletal muscle and mesentery (Figure 3 B,E,C,H and data not shown). Interestingly, *Grip2*, like *Notch3*, displayed preferential expression in arteries (Figure 3C,F). SMC expression of GRIP-2, suspected by *in situ* hybridization analysis, was confirmed by immunohistochemistry using a  $\alpha$ -GRIP-2 specific antibody in combination with the  $\alpha$ -SMA SMC marker (figure 3G-I). Finally, GRIP-2 protein was detected in wild-type brain arteries by immunoblot analysis and found to be strongly downregulated in Notch3KO arteries (Figure 3 J).

### **Grip2 encodes an arterial isoform regulated by the Notch3-RBP-J pathway**

Previously, 3 distinct GRIP-2 isoforms have been described in the rat, including a palmitoylated (pABP-L) and a non-palmitoylated (ABP-L) long variant containing 7 PDZ-domains and a shorter variant (ABP-S) lacking the 7<sup>th</sup> PDZ domain. These 3 variants are generated by alternate leader exon usage (arbitrarily named exon 1b, 1c and 1d) and alternate splicing of exon 21<sup>37</sup>. *In silico* analysis showed that the rat and mouse *Grip2* loci shared the same structure with conserved exons 1b, 1c and 1d located 19.000 to 77.000 bp upstream of exons 2–24 while human *GRIP2* locus exhibited a slightly different structure lacking exon 1c (Figure 4A). Importantly, careful inspection of the databases revealed the existence of an additional GRIP-2 variant in human (NM\_001080423) highly homologous to pABP-L and ABP-L isoforms, but which differs in its N-terminus by the usage of two novel 5' exons, arbitrarily denoted 1a and 1a'. Alignment of the rat and mouse genomic sequences against the human sequence revealed conserved sequences (73–77%) to exon 1a, which had one conserved in-frame ATG codon, whereas sequence of exon 1a' was much more divergent (53–61%) and lacked an inframe ATG in the rat (Figure 4A).

RT-PCR experiments, using sense primers specific of each leader exon against a common antisense primer in the 3'UTR, followed by DNA sequencing of the amplification products, established the existence of 4 distinct transcripts arising from exons 1a, 1b, 1c and 1d in the murine brain or isolated brain arteries. Despite repeated efforts, we were unable to amplify a transcript containing exon 1a'. Remarkably, these 4 transcripts exhibited distinct expression profiles in total brain versus the tail and brain arteries. Exon 1b inclusive transcript (encoding for ABP-L) was abundantly expressed in both the brain and isolated arteries whereas expression of exon 1d and 1a inclusive transcripts encoding for pABP-L and ABP-L<sup>vascular</sup> were essentially restricted to brain and isolated arteries respectively. Exon 1c inclusive transcript (encoding ABP-S) was barely detectable in total brain and vascular tissues (Figure 4B–C).

Next, we assessed the expression of *Grip2* isoforms in the brain arteries of Notch3-null and SM-RBP-J-KO mice. Expression of the ABP-L<sup>vascular</sup> transcript was strongly downregulated in Notch3KO mice and this downregulation was even more pronounced in SM-RBP-J-KO mice. Level of the ubiquitous *ABP-L* variant did not significantly change in Notch3KO and SM-RBP-J-KO mice. Noteworthy, expression of the brain specific *pABP-L* was unchanged or increased in the absence of Notch3 (Figure 4D–G). Together, the results indicate that *Grip2* encodes a vascular isoform, and that the Notch3-RBP-J $\kappa$  pathway preferentially regulates this isoform.

## A *Grip2* mutation in the mouse attenuates myogenic tone in the cerebral arteries

We next considered whether *Grip2* expression in SMC might contribute to arterial SMC maturation/differentiation in maturing brain arteries and myogenic responses within the cerebrovasculature. We analyzed *Grip2*<sup>neo/neo</sup> mice, which have a constitutive disruption of the *Grip2* gene by the insertion of a PGK-neo cassette into exon 3, which encodes for PDZ domain 1. These mice were previously reported to exhibit no overt phenotype<sup>24</sup>.

Analysis of brain artery morphology and SMC structure using high resolution optical microscopy and electron microscopy revealed no overt defect in homozygous *Grip2* mutant mice (n=6) as compared to wild-type littermates (n=5) (Figure 5A–B). One of the important functions of SMC is to maintain arterial blood pressure by regulating the diameter of resistance arteries. We measured systolic and diastolic blood pressure in conscious *Grip2* mutant and control mice, using the tail cuff technique. We found that *Grip2* mutant mice exhibited a moderate but significant reduction in both systolic and diastolic blood pressures, while the heart rate was not altered (Supplemental Figure V). Next, we examined the vasoreactivity and myogenic responses of isolated posterior cerebral arteries from mutant (n=8) and control (n=7) mice. The relaxation to ACh and the contractile responses to PE or KCl were comparable in mutant and control mice (Supplemental Figure VI). In contrast, pressure-induced contraction was markedly attenuated in mutant arteries as compared to control arteries (Figure 5C). For example, at 50 mmHg, myogenic tone was reduced by 35% in the mutant arteries. Because reduced myogenic tone in *Grip2* mutant mice might be caused by an augmented endothelial dilator influence rather than a true reduction in SMC responsiveness, myogenic tone was further measured after pharmacological blockade of the endothelial dilator influence. NO production was inhibited with L-NAME and EDHF-mediated relaxation was inhibited with specific antagonists of Small and Intermediate calcium-activated potassium channels (SK<sub>Ca</sub> and IK<sub>Ca</sub>)<sup>38</sup>. Importantly, myogenic tone remained significantly reduced in *Grip2* mutant mice despite the presence of these inhibitors (Supplemental Figure VII). Thus, our findings reveal a role for GRIP-2 in the control of myogenic responses in the brain arteries. Interestingly, myogenic tone of caudal artery, which expresses 10-fold less *Grip2* mRNA, was unaffected by *Grip2* mutation (Supplemental Figure VIII).

Because of the mild phenotype of *Grip2* mutant mice, we looked whether *Grip1* might compensate for *Grip2* mutation. QRT-PCR showed that *Grip1* transcript level was unaltered in *Grip2* mutant arteries (data not shown). We then tested the hypothesis that introduction of the neo cassette into the *Grip2* gene, which exhibits a complex genomic structure, may not lead to a null allele. QRT-PCR analysis on total RNA prepared from brain or arteries, using a set of primers amplifying all 4 isoforms, showed comparable level of *Grip2* transcript in the mutant and control samples indicating that introduction of the neo cassette did not result in mRNA decay (Supplemental Figure IX-A). Immunoblot analysis of brain and brain arteries lysates, with an antibody raised against the region comprised between the 6<sup>th</sup> and 7<sup>th</sup> PDZ domain of GRIP-2, revealed that homozygous *Grip2* mutant mice lacked the 130-kDa GRIP-2 protein seen in wild-type animals but expressed a shorter ~90-kDa protein, and that *Grip2* heterozygous mice expressed both 130 and ~90-kDa proteins (Supplemental Figure IX-B-C). Thus, these results strongly suggest that the *Grip2* mutation produces a N-terminally truncated GRIP-2 protein, which may behave as a hypomorphic allele and account for the mild phenotype observed in these mice.

## Discussion

It has recently become clear that Notch3 is a major SMC receptor involved in the physiology and pathology of distal arteries, particularly of brain arteries. Here we used constitutive and inducible loss-of-function genetics in combination with inhibitors *in vivo* to investigate the

molecular mechanisms acting downstream of Notch3 in the distal arteries. This effort led to the identification of a core set of novel Notch3-regulated genes in the caudal and cerebral arteries. We establish the requirement of smooth muscle RBP-J $\kappa$  for the expression of Notch3 target genes, indicating that in the context of maturing distal arteries, Notch3 signaling conforms to the canonical RBP-J $\kappa$  pathway. SMC inactivation of RBP-J $\kappa$  in mouse neonates leads to major structural and functional defects within the cerebral arteries of young adult mice that closely resemble those seen in mice constitutively lacking Notch3. Importantly, expression of most of the newly discovered Notch3 targets is significantly diminished in the brain arteries of mice lacking RBP-J $\kappa$  in SMC. Of interest, we find that RBP-J $\kappa$  is required after birth, corroborating our previous observation that maturation of distal arteries predominantly occurs after birth.

Our study uncovers a large number of genes that have not been linked to SMC function before. To provide an example of the functional significance of these genes, we analyzed the *in vivo* role of *Grip2*, which exhibits profound downregulation upon genetic and pharmacologic inactivation of Notch. *Grip2* encodes a multi-PDZ containing protein with an established role in AMPA-receptor trafficking in the neurons. We present several lines of evidence that GRIP-2 functions downstream of Notch3/RBP-J $\kappa$  to regulate myogenic tone in the brain arteries. First, we show that *Grip2* transcript and proteins are detected, in addition to neurons, in SMC of distal arteries including the brain arteries. Second, we find that *Grip2* encodes, in addition to a neuronal isoform, a vascular isoform. Of interest, Notch3/RBP-J $\kappa$  specifically regulates the vascular isoform. Third, we provide evidence that *Grip2* mutant mice, although still expressing a truncated GRIP-2 protein, share phenotypic similarities with mice completely lacking Notch3. Specifically, we show that *Grip2* mutant mice have strongly attenuated myogenic responses in the cerebral arteries. By similarity with Notch3 null mice, this defect is anticipated to compromise cerebral blood flow autoregulation in response to reduction and elevation of systemic arterial blood pressure<sup>7</sup> and AJ, unpublished results. Interestingly, comparative analyses on cerebral arteries versus caudal arteries revealed that these two distal arteries have differential dependency on *Grip2*, which is likely related to differential *Grip2* expression level. Indeed, we found that the caudal artery, which expresses 10-fold less *Grip2* than cerebral arteries, has preserved myogenic tone in *Grip2* mutant mice. Hence, this finding suggests that Notch3, as the other Notch receptors, likely functions using a highly context-dependent set of downstream effectors. We did not find evidence of altered maturation/arterial differentiation of SMC in *Grip2* mutant mice, as seen in Notch3 null mice. However, it is tempting to speculate that mice completely lacking GRIP-2 in SMC might exhibit a more severe vascular phenotype.

How *Grip2* mediates Notch3-dependent myogenic responses in cerebral arteries has yet to be determined. PDZ domains mediate protein-protein interactions by binding to the C termini of its target proteins. In addition to AMPA receptors, GRIP proteins bind various receptors, transmembrane ligands, signaling and cytoskeletal proteins and may act as a scaffold for the assembly of multiprotein signaling complex<sup>39-42</sup>. Among these, NG2 proteoglycan and ephrin-B2 ligand are expressed in SMC and ephrin-B2 ligand is required for SMC to spread and associate with small-diameter blood vessels<sup>43</sup>. Additional studies are required to determine the functional significance of these interactions in the context of cerebral arteries.

Also, the functional significance of the 4 other genes that we identified as immediate and persistent responders to *in vivo* Notch pathway blockade in the brain arteries remains to be clarified. *Xirp1* encodes an F-actin binding protein of unclear function<sup>44</sup> and *Susd5* is structurally related to a protein superfamily containing hyaluronic acid-binding domains<sup>45</sup>. *Nrip2* has been reported to bind and modulate the activity of nuclear receptors including retinoic acid receptor and thyroid hormone receptor<sup>46</sup> and *Pgam2* encodes the muscle



isoform of Phosphoglycerate mutase, an enzyme of the glycolytic pathway that converts glucose into pyruvate<sup>47</sup>.

Our study also uncovers one interesting small group of genes with an established role in SMC function and vessel tone. This group includes *Kv1.5*, which quickly responds to *in vivo* Notch pathway blockade in the brain arteries. *Kv1.5* encodes a pore-forming subunit, which co-assembles with other Kv1  $\alpha$  subunits to form hetero or homotetrameric voltage-gated potassium channels (Kv1). Overexpression in the cerebral arteries of a dominant negative form of Kv1.5 enhances myogenic constriction while overexpression of a wild-type version decreases it<sup>48</sup>. Functionally, Kv1 channels counteract the depolarizing effects of intraluminal pressure and vasoconstrictors, by exerting a hyperpolarizing influence<sup>31</sup>. The other genes include *SIpr3*, which encodes a G-protein coupled receptor. Two recent studies, involving genetic or pharmacological inactivation of *SIpr3*, provide evidence that this receptor is the major contributor to Sphingosine 1 phosphate-induced vasoconstriction in the cerebral circulation<sup>30, 49</sup>. Finally, Phospholamban is a small homopentameric phosphoprotein in the sarcoplasmic reticulum (SR), which regulates SR Ca<sup>2+</sup> load. Nelson and colleagues<sup>50</sup> have established the crucial role of Phospholamban in regulating Ca<sup>2+</sup> uptake into the SR, Ca<sup>2+</sup> spark frequency and thus large-conductance Ca<sup>2+</sup>-activated K<sup>+</sup> (BK) channels activity in SMC of cerebral arteries. Functionally, activation of BK channels, which opposes depolarization of SMC, is one critical negative feedback mechanism responsible for controlling the extent of myogenic constriction, particularly in the brain arteries<sup>51</sup>.

We acknowledge several caveats of *in vivo* studies such as ours. We chose to profile gene expression in whole arteries rather than cultured SMC, which are extremely prone to phenotypic changes. We used the caudal artery, which is the longest distal artery providing sufficient quantity of RNA to synthesize cRNA probes without an amplification step, and in which SMC make up the majority of this vessel. Moreover, our previous work showed that the caudal artery displays the characteristic structural and functional alterations induced by the absence of *Notch3*<sup>7, 10</sup>. While the results show that this strategy yielded biologically relevant Notch3-target genes, we did not fish some recently discovered vascular targets of Notch such as *PDGFR- $\beta$* , *integrin  $\beta$ 3* or *Jagged1*<sup>1920, 52</sup>. This discrepancy could be the result of one or more of the following causes. First, this may reflect the diversity of Notch effectors among different vascular beds. As an example, *Jagged1* has been validated in the maturing aorta<sup>52</sup> and *integrin  $\beta$ 3* in the maturing retinal vessels<sup>20</sup>. Second, this may represent the differences between studies done in cultured cells exposed to transient Notch activation versus the present study done in tissues with persistent Notch inactivation. The latter *in vivo* approach is presumably less appropriate for the discovery of genes exhibiting discrete or transient changes upon manipulation of Notch activity. Moreover, the gene expression profile changes in the Notch3KO mouse model likely integrate compensatory mechanisms. As an example, we found that *HeyL* expression was downregulated in the brain arteries of SM-RBP-J-KO mice and upon GSI treatment whereas it was unchanged in Notch3KO arteries (data not shown). On the other hand, comparison of *in vitro*, *ex vivo* and *in vivo* vascular SMC gene expression profiles indicates that a number of Notch3 targets identified in this study, including for example *Nrip2*, *Kv1.5*, *Grip2*, have their expression almost lost in cultured SMC as early as the first passage (data not shown).

In conclusion, we have carried out *in vivo* genome wide microarray studies using distal arteries from a loss of function *Notch3* mouse model. We validated by quantitative RT-PCR in the tail and brain arteries a core set of 17 Notch3 target genes, including 6 genes which are immediate and persistent responders to *in vivo* Notch blockade in the cerebrovasculature, and established the postnatal requirement of RBP-J $\kappa$  in SMC for their expression. The data indicate that Notch3 transcriptome provides potential for modulating

myogenic response in the brain arteries. As an example, we identified *Kv1.5*, which counteracts the depolarizing effects of intraluminal pressure, and *Grip2*, a novel regulator of myogenic tone. A better understanding of Notch3 signaling promises to provide insight into the basic mechanisms of vSMC biology and myogenic tone regulation in the cerebral arteries. Moreover, by identifying Notch3-regulated transcriptome, this study provides an importance resource of candidate genes for hereditary small-vessel-disease of the brain.

## Supplementary Material

Refer to Web version on PubMed Central for supplementary material.

## Acknowledgments

We are grateful to Dr. Tasuku Honjo for the *RBP-Jk<sup>flox/flox</sup>* mice and to Dr. Stefan Offermanns for the SMMHC-CreER<sup>T2</sup> line.

### Sources of funding

This work was supported by grants from the French National Research Agency (ANR Genopath 2008-RPV08134HSA) and National Institutes of Health (R01 NS054122) to AJ. CF is a recipient of a fellowship from the French Ministry of Education and Research.

## References

- Hill MA, Meininger GA, Davis MJ, Laher I. Therapeutic potential of pharmacologically targeting arteriolar myogenic tone. *Trends Pharmacol Sci.* 2009; 30:363–374. [PubMed: 19541373]
- Iadecola C, Davisson RL. Hypertension and cerebrovascular dysfunction. *Cell Metab.* 2008; 7:476–484. [PubMed: 18522829]
- Pantoni L. Cerebral small vessel disease: From pathogenesis and clinical characteristics to therapeutic challenges. *Lancet Neurol.* 2010; 9:689–701. [PubMed: 20610345]
- Hofmann JJ, Iruela-Arispe ML. Notch signaling in blood vessels: Who is talking to whom about what? *Circ Res.* 2007; 100:1556–1568. [PubMed: 17556669]
- Phng LK, Gerhardt H. Angiogenesis: A team effort coordinated by notch. *Dev Cell.* 2009; 16:196–208. [PubMed: 19217422]
- Fouillade C, Monet-Lepretre M, Baron-Menguy C, Joutel A. Notch signalling in smooth muscle cells during development and disease. *Cardiovasc Res.* 2012
- Domenga V, Fardoux P, Lacombe P, Monet M, Maciazek J, Krebs LT, Klonjowski B, Berrou E, Mericskay M, Li Z, Tournier-Lasserre E, Gridley T, Joutel A. Notch3 is required for arterial identity and maturation of vascular smooth muscle cells. *Genes Dev.* 2004; 18:2730–2735. [PubMed: 15545631]
- Proweller A, Wright AC, Horng D, Cheng L, Lu MM, Lepore JJ, Pear WS, Parmacek MS. Notch signaling in vascular smooth muscle cells is required to pattern the cerebral vasculature. *Proc Natl Acad Sci U S A.* 2007; 104:16275–16280. [PubMed: 17909179]
- Joutel A. Pathogenesis of cadasil: Transgenic and knock-out mice to probe function and dysfunction of the mutated gene, notch3, in the cerebrovasculature. *Bioessays.* 2011; 33:73–80. [PubMed: 20967782]
- Belin de Chantemele EJ, Retailleau K, Pinaud F, Vessieres E, Bocquet A, Guihot AL, Lemaire B, Domenga V, Baufreton C, Loufrani L, Joutel A, Henrion D. Notch3 is a major regulator of vascular tone in cerebral and tail resistance arteries. *Arterioscler Thromb Vasc Biol.* 2008; 28:2216–2224. [PubMed: 18818417]
- Arboleda-Velasquez JF, Zhou Z, Shin HK, Louvi A, Kim HH, Savitz SI, Liao JK, Salomone S, Ayata C, Moskowitz MA, Artavanis-Tsakonas S. Linking notch signaling to ischemic stroke. *Proc Natl Acad Sci U S A.* 2008; 105:4856–4861. [PubMed: 18347334]
- Joutel A, Corpechot C, Ducros A, Vahedi K, Chabriat H, Mouton P, Alamowitch S, Domenga V, Cecillion M, Marechal E, Maciazek J, Vayssiere C, Cruaud C, Cabanis EA, Ruchoux MM,

- Weissenbach J, Bach JF, Bousser MG, Tournier-Lasserre E. Notch3 mutations in cadasil, a hereditary adult-onset condition causing stroke and dementia. *Nature*. 1996; 383:707–710. [PubMed: 8878478]
13. Kopan R, Ilagan MX. The canonical notch signaling pathway: Unfolding the activation mechanism. *Cell*. 2009; 137:216–233. [PubMed: 19379690]
  14. Sanalkumar R, Dhanesh SB, James J. Non-canonical activation of notch signaling/target genes in vertebrates. *Cell Mol Life Sci*. 2010; 67:2957–2968. [PubMed: 20458516]
  15. Heitzler P. Biodiversity and noncanonical notch signaling. *Curr Top Dev Biol*. 2010; 92:457–481. [PubMed: 20816404]
  16. Andersson ER, Sandberg R, Lendahl U. Notch signaling: Simplicity in design, versatility in function. *Development*. 2011; 138:3593–3612. [PubMed: 21828089]
  17. Bray S, Bernard F. Notch targets and their regulation. *Curr Top Dev Biol*. 2010; 92:253–275. [PubMed: 20816398]
  18. Monet M, Domenga V, Lemaire B, Souilhols C, Langa F, Babinet C, Gridley T, Tournier-Lasserre E, Cohen-Tannoudji M, Joutel A. The archetypal r90c cadasil-notch3 mutation retains notch3 function in vivo. *Hum Mol Genet*. 2007; 16:982–992. [PubMed: 17331978]
  19. Jin S, Hansson EM, Tikka S, Lanner F, Sahlgren C, Farnebo F, Baumann M, Kalimo H, Lendahl U. Notch signaling regulates platelet-derived growth factor receptor-beta expression in vascular smooth muscle cells. *Circ Res*. 2008; 102:1483–1491. [PubMed: 18483410]
  20. Schepke L, Murphy EA, Zarpellon A, Hofmann JJ, Merkulova A, Shields DJ, Weis SM, Byzova TV, Ruggeri ZM, Iruela-Arispe ML, Cheresh DA. Notch promotes vascular maturation by inducing integrin-mediated smooth muscle cell adhesion to the endothelial basement membrane. *Blood*. 2012; 119:2149–2158. [PubMed: 22134168]
  21. Han H, Tanigaki K, Yamamoto N, Kuroda K, Yoshimoto M, Nakahata T, Ikuta K, Honjo T. Inducible gene knockout of transcription factor recombination signal binding protein-j reveals its essential role in t versus b lineage decision. *Int Immunol*. 2002; 14:637–645. [PubMed: 12039915]
  22. Wirth A, Benyo Z, Lukasova M, Leutgeb B, Wettschreck N, Gorbey S, Orsy P, Horvath B, Maser-Gluth C, Greiner E, Lemmer B, Schutz G, Gutkind JS, Offermanns S. G12-g13-large-mediated signaling in vascular smooth muscle is required for salt-induced hypertension. *Nat Med*. 2008; 14:64–68. [PubMed: 18084302]
  23. Souilhols C, Cormier S, Monet M, Vandormael-Pournin S, Joutel A, Babinet C, Cohen-Tannoudji M. Nas transgenic mouse line allows visualization of notch pathway activity in vivo. *Genesis*. 2006; 44:277–286. [PubMed: 16708386]
  24. Takamiya K, Kostourou V, Adams S, Jadeja S, Chalepakis G, Scambler PJ, Hagan RL, Adams RH. A direct functional link between the multi-pdz domain protein grip1 and the fraser syndrome protein fras1. *Nat Genet*. 2004; 36:172–177. [PubMed: 14730302]
  25. Soriano P. Generalized lacz expression with the rosa26 cre reporter strain. *Nat Genet*. 1999; 21:70–71. [PubMed: 9916792]
  26. Irizarry RA, Hobbs B, Collin F, Beazer-Barclay YD, Antonellis KJ, Scherf U, Speed TP. Exploration, normalization, and summaries of high density oligonucleotide array probe level data. *Biostatistics*. 2003; 4:249–264. [PubMed: 12925520]
  27. Dong H, Zhang P, Song I, Petralia RS, Liao D, Hagan RL. Characterization of the glutamate receptor-interacting proteins grip1 and grip2. *J Neurosci*. 1999; 19:6930–6941. [PubMed: 10436050]
  28. Joutel A, Monet-Lepretre M, Gosele C, Baron-Menguy C, Hammes A, Schmidt S, Lemaire-Carrette B, Domenga V, Schedl A, Lacombe P, Hubner N. Cerebrovascular dysfunction and microcirculation rarefaction precede white matter lesions in a mouse genetic model of cerebral ischemic small vessel disease. *J Clin Invest*. 2010; 120:433–445. [PubMed: 20071773]
  29. Oloizia B, Paul RJ. Ca<sup>2+</sup> clearance and contractility in vascular smooth muscle: Evidence from gene-altered murine models. *J Mol Cell Cardiol*. 2008; 45:347–362. [PubMed: 18598701]
  30. Salomone S, Potts EM, Tyndall S, Ip PC, Chun J, Brinkmann V, Waeber C. Analysis of sphingosine 1-phosphate receptors involved in constriction of isolated cerebral arteries with receptor null mice and pharmacological tools. *Br J Pharmacol*. 2008; 153:140–147. [PubMed: 18026125]

31. Plane F, Johnson R, Kerr P, Wiehler W, Thorneloe K, Ishii K, Chen T, Cole W. Heteromultimeric kv1 channels contribute to myogenic control of arterial diameter. *Circ Res.* 2005; 96:216–224. [PubMed: 15618540]
32. Krishna K, Redies C. Expression of cadherin superfamily genes in brain vascular development. *J Cereb Blood Flow Metab.* 2009; 29:224–229. [PubMed: 19189440]
33. Guo K, Li J, Wang H, Osato M, Tang JP, Quah SY, Gan BQ, Zeng Q. Prl-3 initiates tumor angiogenesis by recruiting endothelial cells in vitro and in vivo. *Cancer Res.* 2006; 66:9625–9635. [PubMed: 17018620]
34. Liu H, Kennard S, Lilly B. Notch3 expression is induced in mural cells through an autoregulatory loop that requires endothelial-expressed jagged1. *Circ Res.* 2009; 104:466–475. [PubMed: 19150886]
35. Mao L, Takamiya K, Thomas G, Lin DT, Huganir RL. Grip1 and 2 regulate activity-dependent ampa receptor recycling via exocyst complex interactions. *Proc Natl Acad Sci U S A.* 2010; 107:19038–19043. [PubMed: 20956289]
36. Dong H, O'Brien RJ, Fung ET, Lanahan AA, Worley PF, Huganir RL. Grip: A synaptic pdz domain-containing protein that interacts with ampa receptors. *Nature.* 1997; 386:279–284. [PubMed: 9069286]
37. DeSouza S, Fu J, States BA, Ziff EB. Differential palmitoylation directs the ampa receptor-binding protein abp to spines or to intracellular clusters. *J Neurosci.* 2002; 22:3493–3503. [PubMed: 11978826]
38. Cipolla MJ, Smith J, Kohlmeyer MM, Godfrey JA. Skca and ikca channels, myogenic tone, and vasodilator responses in middle cerebral arteries and parenchymal arterioles: Effect of ischemia and reperfusion. *Stroke.* 2009; 40:1451–1457. [PubMed: 19246694]
39. Bruckner K, Pablo Labrador J, Scheiffle P, Herb A, Seeburg PH, Klein R. Ephrin ligands recruit grip family pdz adaptor proteins into raft membrane microdomains. *Neuron.* 1999; 22:511–524. [PubMed: 10197531]
40. Stegmuller J, Werner H, Nave KA, Trotter J. The proteoglycan ng2 is complexed with alpha-amino-3-hydroxy-5-methyl-4-isoxazolepropionic acid (ampa) receptors by the pdz glutamate receptor interaction protein (grip) in glial progenitor cells. Implications for glial-neuronal signaling. *J Biol Chem.* 2003; 278:3590–3598. [PubMed: 12458226]
41. Wyszynski M, Kim E, Dunah AW, Passafaro M, Valtschanoff JG, Serra-Pages C, Streuli M, Weinberg RJ, Sheng M. Interaction between grip and liprin-alpha/syd2 is required for ampa receptor targeting. *Neuron.* 2002; 34:39–52. [PubMed: 11931740]
42. Monea S, Jordan BA, Srivastava S, DeSouza S, Ziff EB. Membrane localization of membrane type 5 matrix metalloproteinase by ampa receptor binding protein and cleavage of cadherins. *J Neurosci.* 2006; 26:2300–2312. [PubMed: 16495457]
43. Foo SS, Turner CJ, Adams S, Compagni A, Aubyn D, Kogata N, Lindblom P, Shani M, Zicha D, Adams RH. Ephrin-b2 controls cell motility and adhesion during blood-vessel-wall assembly. *Cell.* 2006; 124:161–173. [PubMed: 16413489]
44. Otten J, van der Ven PF, Vakeel P, Eulitz S, Kirfel G, Brandau O, Boesl M, Schrickel JW, Linhart M, Hayess K, Naya FJ, Milting H, Meyer R, Furst DO. Complete loss of murine xin results in a mild cardiac phenotype with altered distribution of intercalated discs. *Cardiovasc Res.* 2010; 85:739–750. [PubMed: 19843512]
45. Vicent S, Luis-Ravelo D, Anton I, Garcia-Tunon I, Borrás-Cuesta F, Dotor J, De Las Rivas J, Lecanda F. A novel lung cancer signature mediates metastatic bone colonization by a dual mechanism. *Cancer Res.* 2008; 68:2275–2285. [PubMed: 18381434]
46. Greiner EF, Kirfel J, Greschik H, Huang D, Becker P, Kapfhammer JP, Schule R. Differential ligand-dependent protein-protein interactions between nuclear receptors and a neuronal-specific cofactor. *Proc Natl Acad Sci U S A.* 2000; 97:7160–7165. [PubMed: 10860982]
47. Zhang J, Yu L, Fu Q, Gao J, Xie Y, Chen J, Zhang P, Liu Q, Zhao S. Mouse phosphoglycerate mutase m and b isozymes: Cdna cloning, enzyme activity assay and mapping. *Gene.* 2001; 264:273–279. [PubMed: 11250083]
48. Chen TT, Luykenaar KD, Walsh EJ, Walsh MP, Cole WC. Key role of kv1 channels in vasoregulation. *Circ Res.* 2006; 99:53–60. [PubMed: 16741158]

49. Murakami A, Takasugi H, Ohnuma S, Koide Y, Sakurai A, Takeda S, Hasegawa T, Sasamori J, Konno T, Hayashi K, Watanabe Y, Mori K, Sato Y, Takahashi A, Mochizuki N, Takakura N. Sphingosine 1-phosphate (s1p) regulates vascular contraction via s1p3 receptor: Investigation based on a new s1p3 receptor antagonist. *Mol Pharmacol*. 2010; 77:704–713. [PubMed: 20097776]
50. Wellman GC, Santana LF, Bonev AD, Nelson MT. Role of phospholamban in the modulation of arterial  $Ca^{2+}$  sparks and  $Ca^{2+}$ -activated  $K^{+}$  channels by camp. *Am J Physiol Cell Physiol*. 2001; 281:C1029–1037. [PubMed: 11502581]
51. Ledoux J, Werner ME, Brayden JE, Nelson MT. Calcium-activated potassium channels and the regulation of vascular tone. *Physiology (Bethesda)*. 2006; 21:69–78. [PubMed: 16443824]
52. Manderfield LJ, High FA, Engleka KA, Liu F, Li L, Rentschler S, Epstein JA. Notch activation of jagged1 contributes to the assembly of the arterial wall. *Circulation*. 2012; 125:314–323. [PubMed: 22147907]

\$watermark-text

\$watermark-text

\$watermark-text



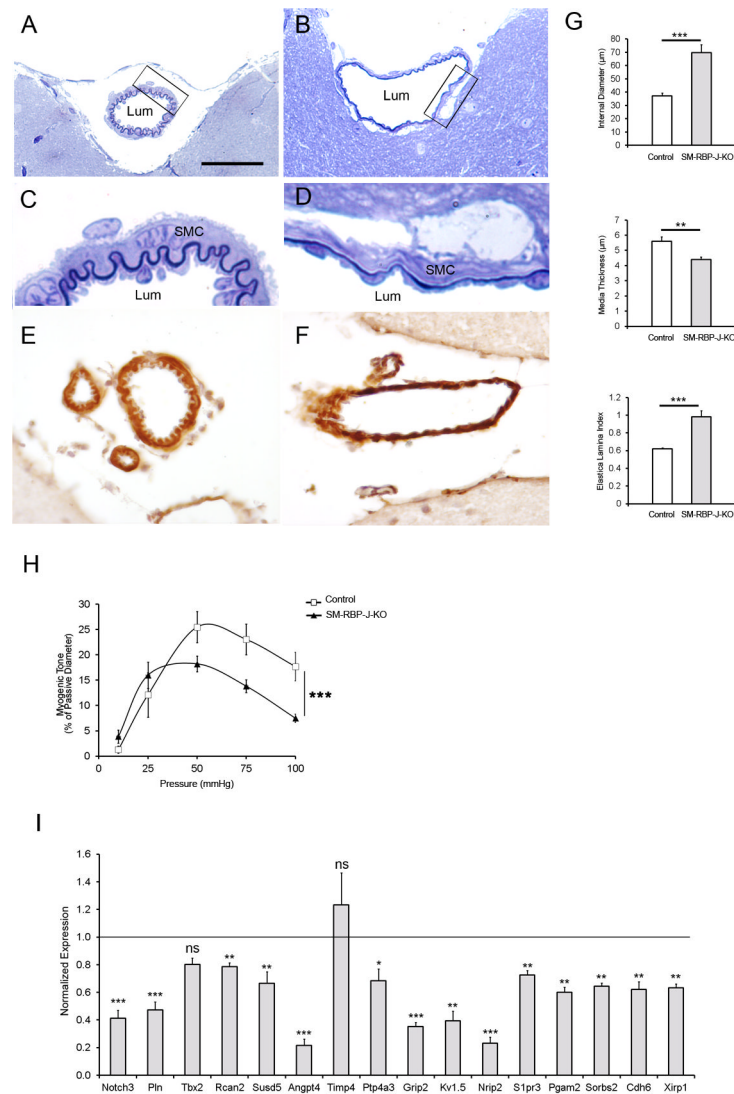


**Figure 1. Structural, functional and molecular defects of brain arteries induced by post-natal deletion of RBP-J $\kappa$  in SMC**

(A–D): Shown are representative semi-thin sections of middle cerebral artery from wild-type (A,C) and SM-RBP-J-KO (B, D) mice stained with Toluidine blue. C and D are magnification of images shown in A and B

(E–F): Shown are brain arteries from wild-type (E) and SM-RBP-J-KO (F) mice immunostained with  $\alpha$ -smooth muscle myosin heavy chain antibody

(G): Quantitative measurement of the internal diameter (top panel), media thickness (medium panel) and elastica lamina index (internal/external perimeter) (bottom panel) in SM-RBP-J-KO (n=5) and control mice (n= 6)

(H): Response of posterior cerebral artery to stepwise increase in pressure (myogenic tone) in wild-type (n= 5) and SM-RBP-J-KO mice (n= 6) shows that myogenic tone is significantly attenuated in mutant mice

(I): QRT-PCR analysis of Notch3 target genes in SM-RBP-J-KO brain arteries, expressed as fold change to control arteries

(\* , p< 0.05; \*\* , p< 0.01 and \*\*\* , p< 0.001). Scale bar 50  $\mu$ m (A,B, E,F) and 10  $\mu$ m in (C–D); Lum, lumen

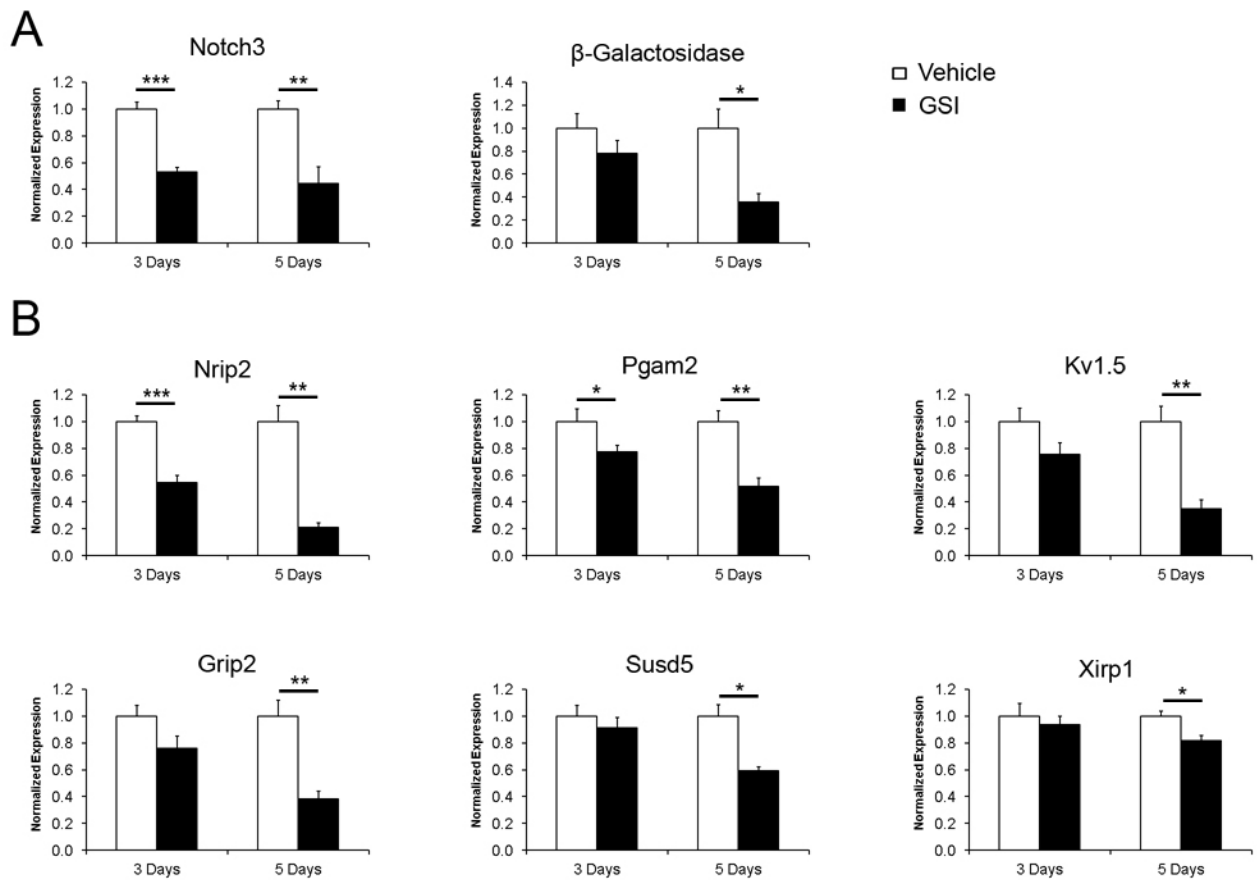


**Figure 2. Transient in vivo pharmacological blockade of Notch signaling leads to downregulation of a subset of Notch3-regulated genes**

QRT-PCR analysis of Notch3 target genes in brain arteries from LY-411575 and vehicle-treated NAS mice. Arteries were collected after 3 and 5 days of treatment. Q-PCR analysis of *Notch3* and  $\beta$ -galactosidase transcripts served as controls to validate Notch signaling blockade (A). Shown are genes exhibiting significant downregulation upon LY-411575 treatment (B)

(\* ,  $p < 0.05$ ; \*\*,  $p < 0.01$  and \*\*\*,  $p < 0.001$ )

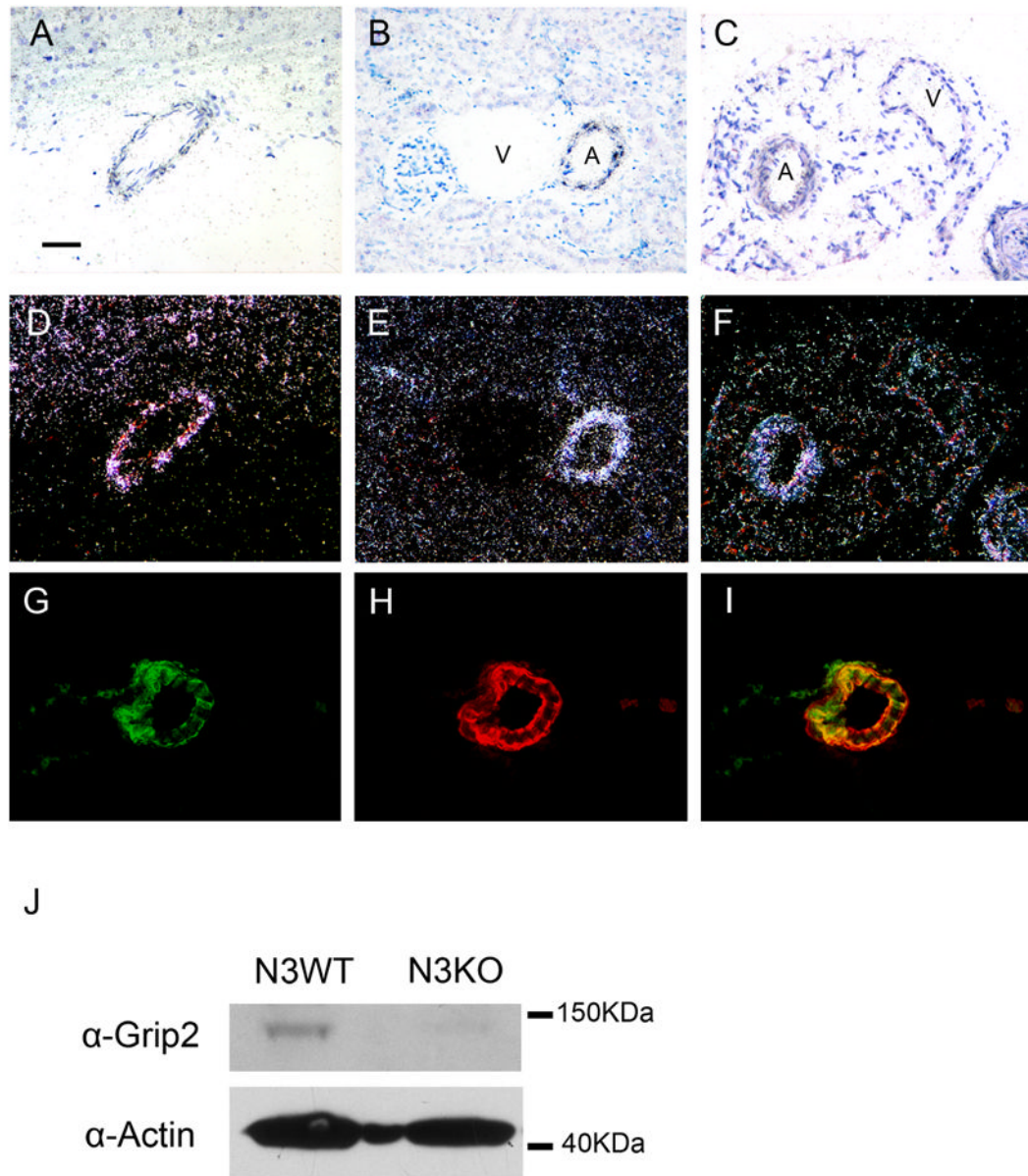


**Figure 3. Grip2 transcript and proteins are detected in arterial smooth muscle cells**

(A–F): *In situ* hybridization with a *Grip2* antisense riboprobe on sections of cortex (A, D), kidney (B, E) and mesentery (C, F) from 1 month-old wild-type mouse. Shown are bright (A–C) and dark field (D–F) images. *Grip2* expression is detected in the vessels with robust signal in the arteries as compared to veins

(G–I): Immunolabeling of brain arteries with antibodies against GRIP-2 (G) and  $\alpha$ -smooth muscle actin

(H) shows that GRIP-2 positive cells overlap with  $\alpha$ -smooth muscle actin positive cells (I, merge)

(J): Representative immunoblot of brain artery lysates prepared from Notch3 wild-type and KO mice probed with the anti- GRIP-2 antibody (upper panel) and the  $\alpha$ -smooth muscle actin antibody (lower panel) shows expression of GRIP-2 into the wild-type artery and reduced expression in the Notch3KO artery

Scale bar 50  $\mu\text{m}$  (A-I); A, artery; V, vein

\$watermark-text

\$watermark-text

\$watermark-text

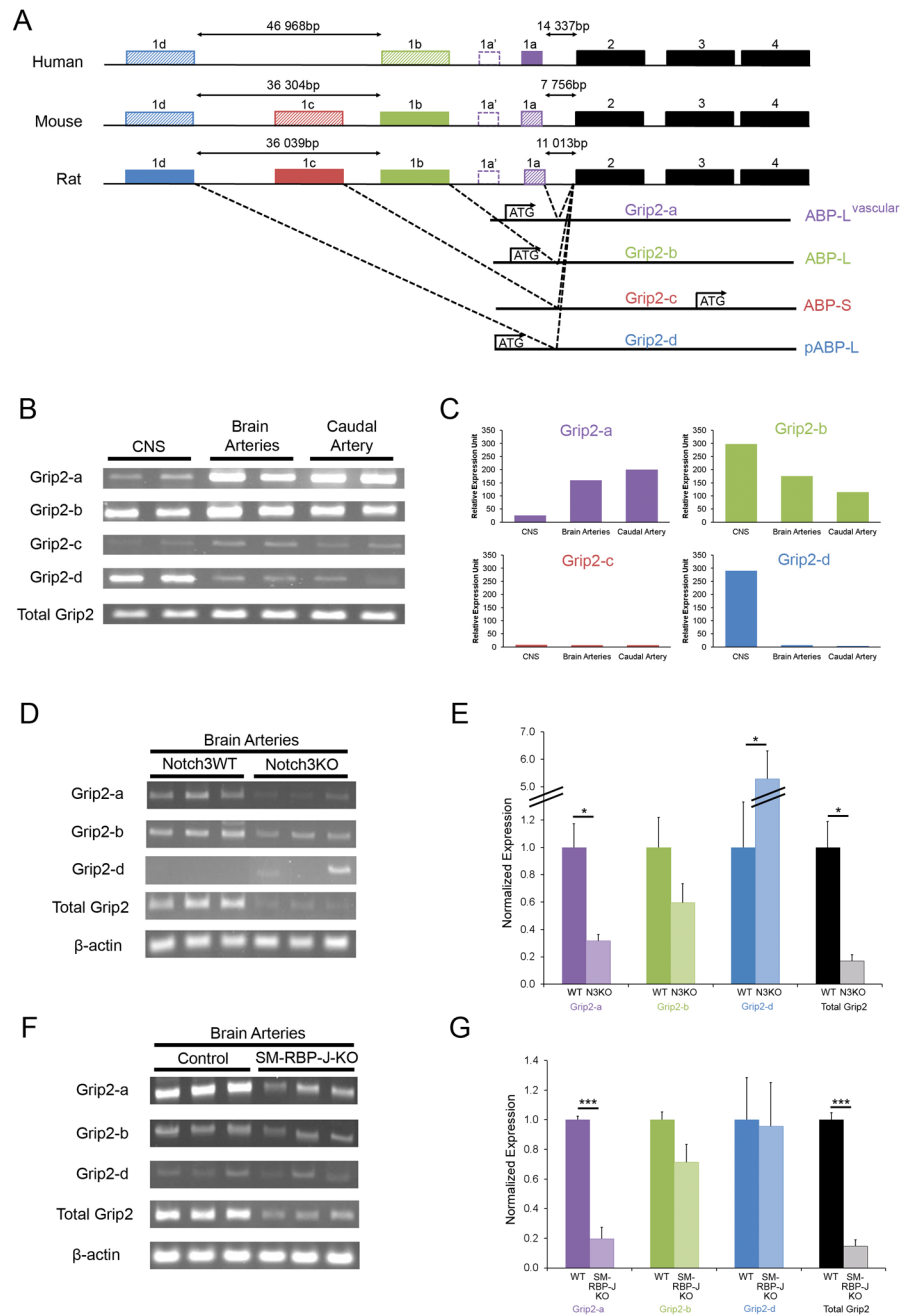


**Figure 4. *Grip2* encodes a vascular isoform which is regulated by Notch3-RBPJ $\kappa$**

(A): Schematic illustration of the *Grip2* locus in human, mouse and rat. Dashed boxes symbolize exons identified through *in silico* analysis

(B–C): RT-PCR analysis of *Grip2* isoforms in total brain, brain arteries and caudal arteries. cDNAs were prepared from 1 $\mu$ g of total RNA of each tissue, amplified with a pair of primers specific of each isoform and separated in agarose gels (B). Expression level of *Grip2* isoforms was normalized against total *Grip2* (C)

(D–E): RT-PCR analysis of *Grip2* isoforms in brain arteries from Notch3KO and control mice. Expression level of *Grip2* isoforms and total *Grip2* was normalized against  $\beta$  actin



(F–G): RT-PCR analysis of *Grip2* isoforms in brain arteries from SM-RBP-J-KO and control mice. Expression level of *Grip2* isoforms and total *Grip2* was normalized against  $\beta$  *actin*

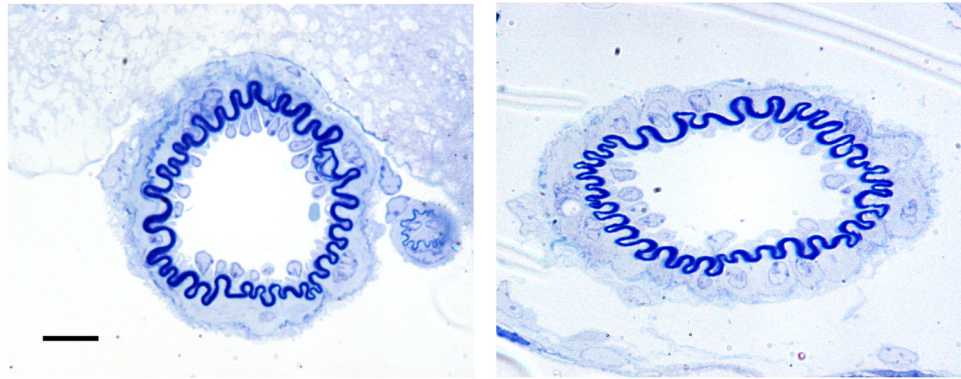
(\* , p< 0.05; \*\* , p< 0.01 and \*\*\* , p< 0.001)

\$watermark-text

\$watermark-text

\$watermark-text

A



B

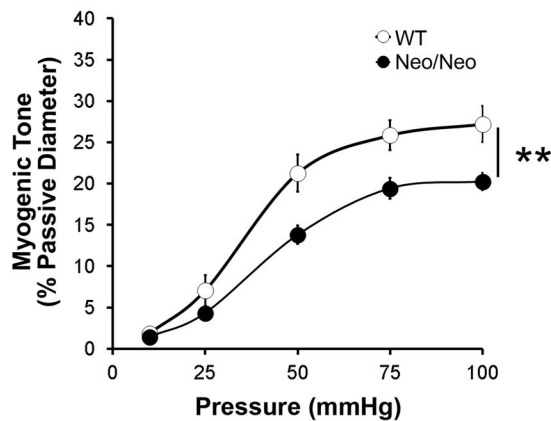


**Figure 5. Brain arteries of *Grip2* mutant mice exhibit normal structure but reduced myogenic responses**

(A–B): Representative semi-thin sections of middle cerebral artery from *Grip2* wild-type (A) and mutant (B) mice stained with Toluidine blue showing no overt structural defect in the mutant artery

Scale bar 10  $\mu$ m (A–B)

(C): Response of cerebral artery to stepwise increase in pressure in wild-type (n=7) and *Grip2* mutant mice (n=8) shows that myogenic tone is significantly attenuated in mutant mice (\*\*,  $p < 0.01$ )

Table 1

List of genes robustly downregulated in Notch3<sup>-/-</sup> distal arteries

Gene Symbol	Gene Name	Microarray Caudal Arteries				qRT-PCR Caudal Arteries				qRT-PCR Brain Arteries			
		FC	p-value*	FC	p-value*	FC	p-value*	FC	p-value*	FC	p-value*	FC	p-value*
<b>Notch3</b>	<b>Notch gene homolog 3 (Drosophila)</b>	<b>0.08</b>	<b>5.65E-05</b>	<b>0.04</b>	<b>0.0004</b>	<b>0.02</b>	<b>0.00009</b>	<b>0.02</b>	<b>0.00009</b>	<b>0.02</b>	<b>0.00009</b>	<b>0.02</b>	<b>0.00009</b>
Perp	PERP, TP53 apoptosis effector	0.23	0.00021	0.12	0.00009	0.86	ns	0.86	ns	0.86	ns	0.86	ns
Pln	phospholamban	0.24	0.00689	0.17	0.03319	0.19	0.00055	0.19	0.00055	0.19	0.00055	0.19	0.00055
Tbx2	T-box 2	0.29	5.21E-05	0.26	0.00067	0.30	0.00005	0.30	0.00005	0.30	0.00005	0.30	0.00005
Rcan2	regulator of calcineurin 2	0.30	0.00015	0.27	0.00289	0.65	0.00424	0.65	0.00424	0.65	0.00424	0.65	0.00424
Susd5	sushi domain containing 5	0.31	0.00036	0.18	0.00062	0.28	0.00001	0.28	0.00001	0.28	0.00001	0.28	0.00001
Angpt4	angiopoietin 4	0.35	0.00603	0.46	0.04180	0.17	0.00034	0.17	0.00034	0.17	0.00034	0.17	0.00034
Timp4	tissue inhibitor of metalloproteinase 4	0.37	7.48E-05	0.44	0.02238	0.73	0.01655	0.73	0.01655	0.73	0.01655	0.73	0.01655
Ptp4a3	protein tyrosine phosphatase 4a3	0.41	0.01003	0.53	0.04781	0.50	0.00295	0.50	0.00295	0.50	0.00295	0.50	0.00295
Grip2	glutamate receptor interacting protein 2	0.42	0.00016	0.17	0.00076	0.15	0.00008	0.15	0.00008	0.15	0.00008	0.15	0.00008
Kcna5 (Kv1.5)	potassium voltage-gated channel, shaker-related subfamily, member 5	0.42	0.00033	0.28	0.00650	0.29	0.00571	0.29	0.00571	0.29	0.00571	0.29	0.00571
Nrip2	nuclear receptor interacting protein 2	0.47	0.00155	0.42	0.00938	0.36	0.00550	0.36	0.00550	0.36	0.00550	0.36	0.00550
S1pr3	sphingosine-1-phosphate receptor 3	0.48	0.00675	0.55	0.03307	0.33	0.00137	0.33	0.00137	0.33	0.00137	0.33	0.00137
Pgam2	phosphoglycerate mutase 2	0.49	0.00227	0.57	ns	0.42	0.00179	0.42	0.00179	0.42	0.00179	0.42	0.00179
Hp	haptoglobin	0.50	0.00167	0.67	0.04086	1.06	ns	1.06	ns	1.06	ns	1.06	ns
Sorbs2	sorbin and SH3 domain containing 2	0.53	0.00240	0.43	0.00250	0.33	7.18E-07	0.33	7.18E-07	0.33	7.18E-07	0.33	7.18E-07
Cdh6	cadherin 6	0.54	0.00191	0.55	0.00021	0.62	0.02394	0.62	0.02394	0.62	0.02394	0.62	0.02394
Xirp1	xin actin-binding repeat containing 1	0.56	0.00638	0.44	0.00493	0.19	0.01111	0.19	0.01111	0.19	0.01111	0.19	0.01111

\*, Student t-test